Influence of the Ambient Relative Humidity on the Very-Long-Term DEF

Thierry Houndonougbo, Boumediene Nedjar, Loic Divet, Jean-Michel Torrenti

construction materials

MDPI

Communication

Influence of the Ambient Relative Humidity on the Very-Long-Term DEF

Thierry Houndonougbo [1], Boumediene Nedjar [2], Loic Divet [1] and Jean-Michel Torrenti [3,4,*]

[1] Physical and Chemical Properties and Durability of Materials Laboratory (CPDM), Department of Materials and Structures (MAST), Université Gustave Eiffel, 5 Boulevard Descartes, CEDEX 2, 77454 Marne-la-Vallée, France; thierry.houndonougbo@univ-eiffel.fr (T.H.); loic.divet@outlook.com (L.D.)
[2] Urban and Civil Engineering Testing and Modeling Laboratory (EMGCU), Department of Materials and Structures (MAST), Université Gustave Eiffel, 5 Boulevard Descartes, CEDEX 2, 77454 Marne-la-Vallée, France; boumediene.nedjar@univ-eiffel.fr
[3] Sustainable Building Materials Laboratory (UMR MCD), Department of Materials and Structures (MAST), Université Gustave Eiffel, 5 Boulevard Descartes, CEDEX 2, 77454 Marne-la-Vallée, France
[4] ESITC-Paris, 79 Avenue Aristide Briand, 94110 Arcueil, France
* Correspondence: jean-michel.torrenti@univ-eiffel.fr

Abstract: Relative humidity is a key parameter for the development of delayed ettringite formation (DEF). Here, new results of very-long-term experiments (10 years) are presented. It is observed that for a relative humidity of 96%, swelling could occur after several years but with a slower kinetics. A model coupling the kinetics of swelling with the internal relative humidity is presented. It is shown that this model can reproduce the experimental behavior.

Keywords: concrete; delayed ettringite formation; relative humidity; modelling

Citation: Houndonougbo, T.; Nedjar, B.; Divet, L.; Torrenti, J.-M. Influence of the Ambient Relative Humidity on the Very-Long-Term DEF. *Constr. Mater.* **2023**, *3*, 405–413. https://doi.org/10.3390/constrmater3040026

Received: 9 August 2023
Revised: 17 October 2023
Accepted: 30 October 2023
Published: 10 November 2023

1. Introduction

Delayed ettringite formation (DEF) is a pathology that can affect massive concrete structures when high temperatures occur at an early age [1]. The risk is particularly important in the case of nuclear power plant containments [2,3].

The influence of the nature and mineralogical composition of cements on DEF has been widely demonstrated in the literature [4–7]. Portland cement of the CEM I type is the most reactive, depending on three main elements: sulfates, aluminates, and alkalis. The influence of their content in cement on DEF has been the subject of numerous studies [1,7].

Substituting part of the cement with mineral additions (blast furnace slag, fly ash, silica fume, or metakaolin) is effective in limiting or even inhibiting the internal sulfate reaction [8–10].

It is also well known and accepted that high humidity is needed for the development of DEF [3–12]. Indeed, ettringite formation is very water-intensive (32 molecules of water per molecule of ettringite). As a result, the occurrence of DEF is directly conditioned by a high water content in the material and, consequently, a high relative humidity in the storage environment. Furthermore, Collepardi [5] explains that water also plays a role in the ionic transport necessary for the reaction. Thiebaut [11] points out that DEF only appears in humid environments, where the material is subject to significant external water inputs. In situ observations support this view, highlighting a more common occurrence of degradation in parts of structures subjected to higher water inflows [8,12,13]. An increase in water content would thus lead to an increase in expansion due to RSI [14–19].

However, it seems difficult to find a consensus in the literature regarding the relative humidity threshold above which the risk of DEF is indisputable. Martin [20] defines this threshold at 95%, while Al Shamaa et al. [21] estimate it at 98% with very slow swelling. However, Graf-Noriega [22] reveals that after 4 years of monitoring, below 92%, no expansion was detected, whereas swelling seemed to develop freely above this threshold.

Heinz and Ludwig [16], for their part, did not observe swelling in specimens stored below 90% relative humidity, nor did Shimada et al. in [18].

Concerning modeling, Sellier and Multon [23] proposed a highly nonlinear function to express the influence of the internal relative humidity on the kinetics of DEF. They adjusted this function to obtain a good correlation with Al Shamaa's results. They explain this influence by the need for water for the reaction and diffusion of the reactants. When the saturation decreases, diffusion slows down very rapidly. As in the case of thermal heating, DEF seems to develop retroactively with relative humidity [22]. Thus, samples that showed no swelling when subjected to 91% relative humidity began to swell when subsequently immersed, with the same evolution as the specimens immersed at the outset [21,24]. The same findings occurred using specimens from Heinz and Ludwig [16] initially at 90% relative humidity.

Recently, Martin et al. [25] started a new program of tests at 75%, 88%, 92%, 96%, and 100% relative humidities with wetting–drying cycles, but the results are not yet available. Al Shamaa in [21] has performed tests at 91%, 94%, 96%, and 98%. After more than 3 years, the samples that were stored below 96% did not show significant swelling. The samples stored at 94% were kept under this condition, and we present here the very-long-term behavior of these samples. Accidentally, the measurements were stopped for the samples at a relative humidity RH = 96%.

After a presentation of the experimental results including a discussion of the real exposure conditions, the possible modeling of the long-term swelling of concrete subjected to DEF in a variable relative humidity is discussed and compared to the experimental results.

2. Experiments

2.1. Materials, Specimens Curing, and Storage

Materials, curing, and storage conditions were presented in the previous paper concerning the influence of the relative humidity on DEF [21]. The mix (given in Table 1) was designed to favor an expansive behavior [25,26]. Particularly, the cement was a Portland cement (CEM I) with large sulfate and alkali contents, which are major factors for DEF. Additions like slag, fly ash, or silica fume that could mitigate DEF were not used. A heat treatment, where the temperature was maintained at 80 °C for 3 days, was applied. The total duration of the heat treatment was 7 days. This treatment was representative of the temperature history in a massive concrete structure at early age like a raft foundation of a nuclear power plant [21]. Tests were performed on cylinders of 11 cm in diameter and 22 cm in height.

Table 1. Concrete composition.

Material	kg/m^3
Cement CEM I 52.5 N	400
Siliceous sand 0/4	710
Siliceous aggregate 4/20	1090
Water	190

After the heat treatment, the specimens were stored at 20 °C in different conditions: in tap water and at RH = 100%, and controlled RH approximately equal to 91%, 94%, and 98% through different saturated salts solutions chosen from the available data [27] and at a temperature close to 20 °C.

The nomenclature of the tests is as follows:

- Im for concretes that were immersed continuously in water;
- RH94, RH98, and RH100 for concretes that were stored initially at 94%, 98%, and 100% RH, respectively.

In the previous study, the samples were followed for 1000 days. The samples concerning the RH equal to 94% and stored over a solution of potassium chloride were kept to follow the long-term behavior (because in the case of higher RH, final swelling was observed, and the sample with RH = 91% was used to show that swelling could be initiated by placing the specimen into water [21]).

2.2. Measurements

Axial expansion of the concrete specimens was monitored routinely with a digital extensometer that measured the length between the steel studs glued on three locations placed at 120 degrees around the diameter (see [21] for a complete description).

The measurements of the relative humidity of the storage were lost during the period between 1250 days and 3200 days. Only recent measurements of the RH complete the old ones (Figure 1). These recent measurements (see Figure 1) were performed using a data logger for humidity and temperature (Rotronic Hydrolog HL-NT) that was placed 5 cm over the specimen. The humidity probe was calibrated using standard solutions at 50% RH and 95% RH. Over two months, the relative humidity varied slightly (due to temperature variations) between 95 and 96.4% with an average of 95.5%. In previous measurements [21], the average RH was 94%. We can therefore estimate that, during the later period (between 1250 days and 3200 days), the RH increased from 94% to 96%. It is not possible to be more precise.

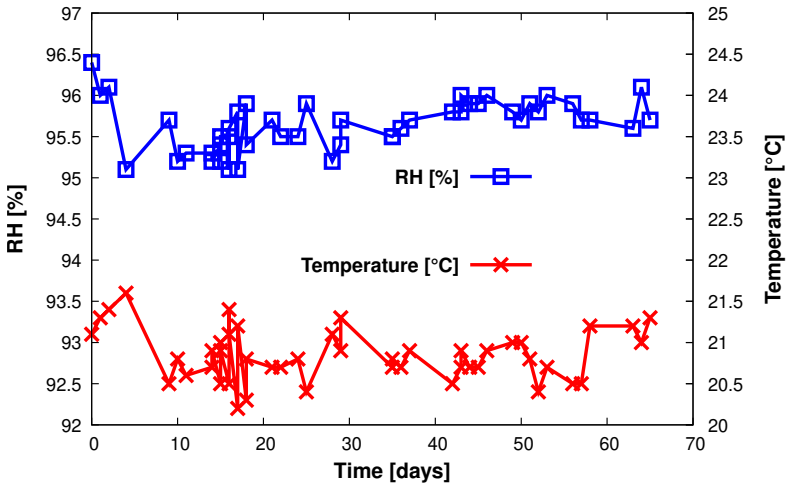

Figure 1. Recent measurements of the relative humidity and the temperature.

2.3. Results

Figure 2 shows the expansion curves obtained for the different concrete storage conditions. The results confirm that the relative humidity has a strong influence on the expansion due to DEF. In our previous study [21], none of the concretes that were stored at 96% and 94% RH presented significant swelling after 1250 days of storage. Now, it is possible to observe that, after 3200 days of storage, for 96% RH (specimen initially at 94% RH), an important swelling was observed after a very long period of incubation. Maybe, for a lower RH, this period is longer. That would be very difficult to demonstrate in laboratory conditions due to the duration of the tests or the in situ conditions, due to the variations in the environmental relative humidity.

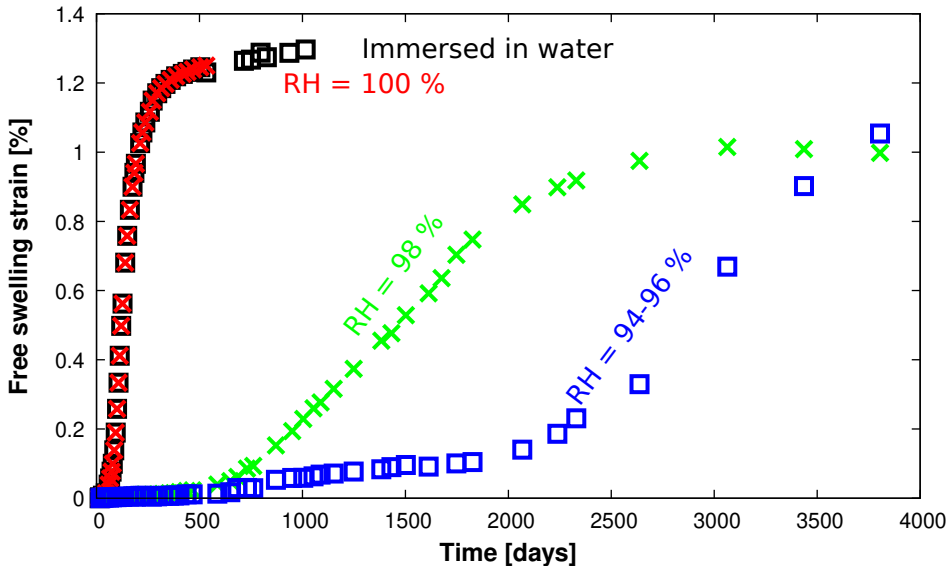

Figure 2. Expansions of all the concrete specimens at different humidities.

3. Modeling

Within the continuum thermodynamics framework, it can be deduced from the mathematical developments in [28] that the swelling evolution equation can be expressed as follows, see also [29]:

$$\tau_c\,\varepsilon_\infty^0\left(1+e^{\frac{\tau_l}{\tau_c}}\right)\dot{\varepsilon}_\chi \;+\; \left(e^{\frac{\tau_l}{\tau_c}}\right)\varepsilon_\chi^2 \;+\varepsilon_\infty^0\left(1-e^{\frac{\tau_l}{\tau_c}}\right)\varepsilon_\chi \;=\; \left(\varepsilon_\infty^0\right)^2, \tag{1}$$

where the evolving variable ε_χ is the chemically expanding strain. The dot notation $\dot{\varepsilon}_\chi$ refers to the derivative of the quantity ε_χ with respect to time t. Equation (1) depends on three parameters:

- The stress-free potential chemical strain ε_∞^0 that constitutes the amplitude of fully reached expansion ;
- The characteristic time τ_c ;
- The latency time τ_l.

The two latter parameters characterize the kinetics of expansion with a typical S-shaped form for the chemical expansion function $\varepsilon_\chi(t)$.

For fixed environmental conditions, the solution of the above differential equation is exactly the Larive's relation [30] that is widely used in the literature; see, for example [25,31], among many others:

$$\varepsilon_\chi(t) \;=\; \varepsilon_\infty^0\,\frac{1-e^{-\frac{t}{\tau_c}}}{1+e^{-\frac{t+\tau_l}{\tau_c}}}. \tag{2}$$

The details about this solution procedure are given in Appendix A.

Now, when the hydric conditions are of different RH values, we suppose that the evolution Equation (1) is still valid but this time with hydric-dependent parameters. Observe from Figure 2 that the curves have the same shape but widen as the humidity decreases.

Among the possible choices, and for the sake of simplicity, we consider in this work that only the characteristic and latency times are RH-dependent. We choose the following forms:

$$\begin{aligned} \tau_c(RH) &= \tau_c^{100}\Big(1+a_c(1-RH)^{b_c}\Big) \\ \tau_l(RH) &= \tau_l^{100}\Big(1+a_l(1-RH)^{b_l}\Big) \end{aligned} \quad , \tag{3}$$

where τ_c^{100} and τ_l^{100} are, respectively, the characteristic and latency times for fully saturated concrete at $RH = 100\% \equiv 1$; i.e., $\tau_c(RH = 100\%) = \tau_c^{100}$ and $\tau_l(RH = 100\%) = \tau_l^{100}$, and a_c, b_c, a_l, and b_l are material parameters to be identified from the above test results. With the choices in (3), the characteristic times increase with decreasing RH.

For the general case of variable hydric conditions with time, Appendix B gives details of a possible approximation using an exponential map algorithm.

From the test results of Figure 2, we identify the set of parameters summarized in Table 2. Figure 3 shows the numerical results predicted by the model for different exposures to humidity. For the sake of comparison, they are superposed to the corresponding experimental data (in dashed lines). The comparison shows the ability of the model to reproduce the experimental results with reasonable accuracy.

Table 2. Identified material parameters.

Material Parameters			
Potential chemical strain (%)	$\varepsilon_\infty^0 = 1.1965$	–	–
Characteristic time, Equation (3)	$\tau_c^{100} = 33.1$ days	$a_c = 31$	$b_c = 0.25$
Latency time, Equation (3)	$\tau_l^{100} = 120.14$ days	$a_l = 150$	$b_l = 0.65$

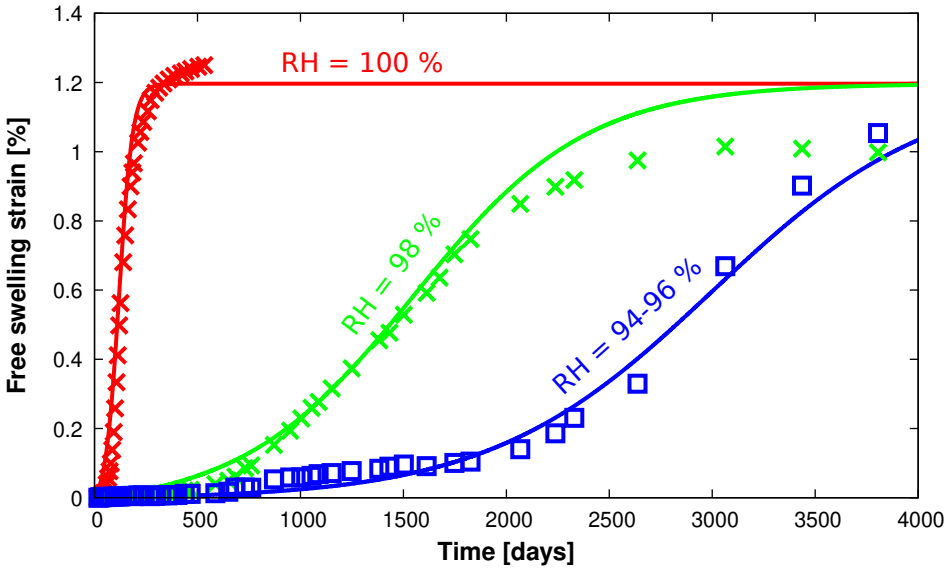

Figure 3. Simulated expansions of concrete specimens exposed to different relative humidity (solid lines). Superposition with the experimental data (dashed lines).

4. Discussion

In our experiment, DEF developed at an RH close to 96%. This proves that the DEF trigger threshold is at least equal to this value. But, it does not imply that for a lower value of the RH and a longer test period, DEF could not be developed.

It appears also that, once the reaction has started, the swelling that will eventually be achieved is just as great as with a sample directly immersed in water. However, the kinetics is slower. This could be explained by the fact that to obtain ettringite precipitation, water is

a reactant, and ions should diffuse in the pore solution to react [23]. The consequence is a highly nonlinear variation in the parameters of the model governing the swelling.

As a result, when modeling a structure affected by DEF, coupling with a drying model will be very important. The model will also have to incorporate the dependence of the kinetic development of the reaction on the internal relative humidity of the concrete.

With the proposed model, which takes these considerations into account, it is possible to reproduce the experimental results with correct accuracy. Another approach is, of course, possible using a different model [23]. These models will allow simulation of a real structure. In this case, the cyclic drying and wetting conditions will have to be considered, which was not the case here [31].

Note that our results were obtained on concrete made with a CEM I cement with a large content of sulfates and alkali. With the use of additions that could mitigate the reaction, it is possible to observe a different behavior.

5. Conclusions

In this paper, we presented an extension of the experimental results concerning the very-long-term swelling of concrete samples affected by DEF. The total duration of the tests exceeded 10 years. The samples initially stored at 94% RH finally showed a swelling. But, the actual measured RH was closer to 96%. So, it can be concluded that, at this level of internal humidity, DEF finally occurs but with slow kinetics. This implies a nonlinear relation between the relative humidity and the swelling due to DEF. From our results, it cannot be deduced whether there is a threshold for the relative humidity below which DEF never occurs, or whether there is a very long delay before the swelling starts.

Furthermore, we have presented an efficient tool for the modeling of the influence of the relative humidity on DEF expansion, i.e., here, with RH-dependent characteristics and latency times. From the numerical point of view, we have presented an algorithmic design that, for instance, could be used in the context of a finite element framework.

The numerical simulations have shown the ability of the model to reproduce the experimental results issued from the very-long-term experimental campaign. However, further studies are ongoing to include this evolution law within constitutive modeling including the coupling with other mechanical phenomena such as creep, plasticity, and mechanical damage, these latter being respectively described with the usual internal variables $\boldsymbol{\varepsilon}^{\mathrm{cr}}$, $\boldsymbol{\varepsilon}^{\mathrm{p}}$ and the scalar d, i.e., in a form $\boldsymbol{\sigma} = \boldsymbol{H}(d) : (\boldsymbol{\varepsilon} - \boldsymbol{\varepsilon}_{\chi} - \boldsymbol{\varepsilon}^{\mathrm{cr}} - \boldsymbol{\varepsilon}^{\mathrm{p}})$, where $\boldsymbol{\sigma}$ is the stress tensor, $\boldsymbol{\varepsilon}$ is the total strain, and $\boldsymbol{H}(d)$ is the damage-dependent elasticity tensor (Hooke's law). Hence, the above evolution Equation (1) is only the part that describes the evolution of the internal variable relative to swelling $\boldsymbol{\varepsilon}_{\chi}$, and that must be appended to the stress–strain relation. Furthermore, the application of the model to real structures will also be interesting to see if it could explain a part of the structural size effect of DEF [32].

Author Contributions: T.H. Resources, Revision, Validation, B.N. Writing, writing-revise, editing, numerical modeling, L.D. Resources, writing-revise and editing, Validation, J.-M.T. Conceptualization, Methodology, Validation, data curation, writing and editing. All authors have read and agreed to the published version of the manuscript.

Funding: This research received no external funding

Data Availability Statement: Data available on request from the authors

Conflicts of Interest: The authors declare no conflict of interest.

Appendix A. Swelling Evolution in the Case of Constant *RH*

In the case of constant relative humidity, the solution of the evolution Equation (1) can be determined analytically as follows. Let us rewrite Equation (1) as

$$\frac{(1+\alpha)\tau_c}{\varepsilon_{\infty}^{0}}\,\dot{\varepsilon}_{\chi} + \left(\frac{\varepsilon_{\chi}}{\varepsilon_{\infty}^{0}}\right)^{2} + (\alpha-1)\,\frac{\varepsilon_{\chi}}{\varepsilon_{\infty}^{0}} = \alpha, \tag{A1}$$

where, for convenience, we have introduced the notation $\alpha = e^{-\frac{\tau_l}{\tau_c}}$.

By noticing that (A1) is equivalently given by

$$\begin{aligned} \frac{(1+\alpha)\tau_c}{\varepsilon^0_\infty}\frac{d\varepsilon_\chi}{dt} &= -\left(\frac{\varepsilon_\chi}{\varepsilon^0_\infty}\right)^2 + (1-\alpha)\frac{\varepsilon_\chi}{\varepsilon^0_\infty} + \alpha \\ &\equiv -\left(\frac{\varepsilon_\chi}{\varepsilon^0_\infty}+\alpha\right)\left(\frac{\varepsilon_\chi}{\varepsilon^0_\infty}-1\right) \end{aligned}, \tag{A2}$$

this allows a separation of variables as

$$\begin{aligned} -\frac{dt}{(1+\alpha)\tau_c} &= \frac{\varepsilon^0_\infty\, d\varepsilon_\chi}{(\varepsilon_\chi+\alpha\varepsilon^0_\infty)(\varepsilon_\chi-\varepsilon^0_\infty)} \\ &\equiv \frac{d\varepsilon_\chi}{(1+\alpha)(\varepsilon_\chi-\varepsilon^0_\infty)} - \frac{d\varepsilon_\chi}{(1+\alpha)(\varepsilon_\chi+\alpha\varepsilon^0_\infty)} \end{aligned}. \tag{A3}$$

An easy integration then gives

$$\varepsilon_\chi(t) = \varepsilon^0_\infty \frac{1+\alpha C e^{-\frac{t}{\tau_c}}}{1-Ce^{-\frac{t}{\tau_c}}}, \tag{A4}$$

where the constant C is deduced from the initial condition. Here, as the relative humidity is constant, we have $\varepsilon_\chi(t=0)=0$, which gives $C=-1/\alpha$ that, when replaced back into Equation (A4), leads to Larive's relation (2).

Appendix B. Swelling Evolution in the Case of Variable *RH*

In the case of variable relative humidity with time, i.e. $RH \equiv RH(t)$, the evolution Equation (1) can still be used. Here, we give an algorithmic design for its numerical approximation with an exponential map. Within a typical time interval $[t_n, t_{n+1}]$, we consider as known the expanding strain ε_{χ_n} at time t_n. The update to its new value $\varepsilon_{\chi_{n+1}}$ at time t_{n+1} is performed as follows:

At time t_{n+1}, the relative humidity is assumed to be known, $RH(t_{n+1}) \equiv RH_{n+1}$, and hence also the material parameters:

$$\tau_{c_{n+1}} = \tau_c(RH_{n+1}), \quad \tau_{l_{n+1}} = \tau_l(RH_{n+1}), \quad \varepsilon^0_{\infty_{n+1}} = \varepsilon^0_\infty(RH_{n+1}), \tag{A5}$$

where for the first two, the relations (3) are to be used, and for the third one, an RH-dependence can be allowed.

The construction of the algorithm starts from the above Equation (A4), this time with the constant C deduced from the initial condition:

$$\varepsilon_\chi(t=t_n) = \varepsilon_{\chi_n}, \tag{A6}$$

which gives

$$C = \frac{\varepsilon_{\chi_n} - \varepsilon^0_{\infty_{n+1}}}{\varepsilon_{\chi_n} + \alpha_{n+1}\,\varepsilon^0_{\infty_{n+1}}} e^{\frac{t_n}{\tau_{c_{n+1}}}}, \tag{A7}$$

where $\alpha_{n+1} = e^{-\frac{\tau_{l_{n+1}}}{\tau_{c_{n+1}}}}$.

Replacing (A7) into (A4) gives then:

$$\varepsilon_{\chi_{n+1}} = \frac{\varepsilon_{\chi_n} + \alpha_{n+1}\,\varepsilon^0_{\infty_{n+1}} + (\varepsilon_{\chi_n} - \varepsilon^0_{\infty_{n+1}})\alpha_{n+1}\,e^{-\frac{\Delta t}{\tau_{c_{n+1}}}}}{\varepsilon_{\chi_n} + \alpha_{n+1}\,\varepsilon^0_{\infty_{n+1}} - (\varepsilon_{\chi_n} - \varepsilon^0_{\infty_{n+1}})\,e^{-\frac{\Delta t}{\tau_{c_{n+1}}}}}\,\varepsilon^0_{\infty_{n+1}}, \tag{A8}$$

where $\Delta t = t_{n+1} - t_n$.

The exponential map (A8) is useful in a finite element implementation, in which case this update would be conducted at the level of the integration points.

References

1. Taylor, H.F.W.; Famy, C.; Scrivener, K.L. Delayed ettringite formation. *Cem. Concr. Res.* **2001**, *31*, 683–693. [CrossRef]
2. Al Shaama, M.; Lavaud, S.; Divet, L.; Nahas, G.; Torrenti, J.M. Coupling between mechanical and transfer properties and expansion due to DEF in a concrete of nuclear power plant. *Nucl. Eng. Des.* **2014**, *266*, 70–77. [CrossRef]
3. Rasheed, P.A.; Nayar, S.K.; Barsoum, I.; Alfantazi, A. Degradation of concrete structures in nuclear power plants: A review of the major causes and possible preventive measures. *Energies* **2022**, *15*, 8011. [CrossRef]
4. Scrivener, K.L.; Damidot, D.; Famy, C. Possible mechanisms of expansion of concrete exposed to elevated temperatures during curing (also known as DEF) and implications for avoidance of field problems. *Cem. Concr. Aggreg.* **1999**, *21*, 93–101.
5. Collepardi, M. A state-of-the-art review on delayed ettringite attack on concrete. *Cem. Concr. Compos.* **2003**, *25*, 401–407. [CrossRef]
6. Salgues, M.; Sellier, A.; Multon, S.; Bourdarot, E.; Grimal, E. DEF modelling based on thermodynamics equilibria and ionic transfers for structural analysis. *Eur. J. Environ. Civ. Eng.* **2014**, *18*, 377–402.
7. Pavoine, A.; Brunetaud, X.; Divet, L. The impact of cement parameters on Delayed Ettringite Formation. *Cem. Concr. Compos.* **2012**, *34*, 521–528. [CrossRef]
8. Lawrence, C.D. Long-term expansion of mortars and concretes. *Spec. Publ.* **1999**, *177*, 105–124.
9. Miller, F.M.; Conway, T. Use of ground granulated blast furnace slag for reduction of expansion due to delayed ettringite formation. *Cem. Concr. Aggreg.* **2003**, *25*, 221–230.
10. Ramlochan, T.; Zacarias, P.; Thomas, M.D.A.; Hooton, R.D. The effect of pozzolans and slag on the expansion of mortars cured at elevated temperature: Part I: Expansion behaviour. *Cem. Concr. Res.* **2003**, *33*, 807–814. [CrossRef]
11. Thiebaut, Y.; Multon, S.; Sellier, A.; Lacarriere, L.; Boutillon, L.; Belili, D.; Hadji, S. Effects of stress on concrete expansion due to delayed ettringite formation. *Constr. Build. Mater.* **2018**, *183*, 626–641. [CrossRef]
12. Boening, A.; Funez, L.M.; Memberg, L.; Roche, J.; Tinkey, B.; Kligner, R.E.; Fowler, T.J. Structural assessment of bridges with premature concrete deterioration due to expansive reactions. *ACI Struct. J.* **2014**, *106*, 196–204.
13. Mielenz, R.C.; Marusin, S.L.; Hime, W.G.; Jugovic, Z.T. Investigation of prestressed concrete railway tier distress. *Concr. Int.* **1995**, *17*, 62–68.
14. Hanehara, S.; Omayada, T.; Fujiwara, T. Reproduction of delayed ettringite formation in concrete and its mechanism. In Proceedings of the International Conference on Microstructure Related Durability of Cementitious Composites, Nanjing, China, 13–15 October 2008; RILEM Publications: Bagneux, France, 2008.
15. Famy, C.; Scrivener, K.L.; Atkinson, A.; Brough, A.R. Influence of the storage conditions on the dimensional changes of heat-cured mortars. *Cem. Concr. Res.* **2001**, *31*, 795–803. [CrossRef]
16. Heinz, D.; Kalde, M.; Ludwig, U.; Ruediger, I. Present state of investigation on damaging late ettringite formation (DEF) in mortars and concretes. In *SP177: Ettringite—The Sometimes Host of Destruction*; Erlin, B., Ed.; American Concrete Institute: Farmington Hills, MI, USA, 1999; pp. 1–14.
17. Rust, C.K. Role of Relative Humidity in Concrete Expansion due to Alkali-Silica Reaction and Delayed Ettringite Formation: Relative Humidity Thresholds, Measurement Methods, and Coating to Mitigate Expansion. Ph.D. Thesis, University of Texas, Austin, TX, USA, 2009.
18. Shimada, Y.; Johansen, V.C.; Miller, F.M.; Mason, T.O. *Chemical Path of Ettringite Formation in Heat-Cured Mortar and Its Relationship to Expansion: A Literature Review*; Portland Cement Association: Skokie, IL, USA, 2005.
19. Older, I.; Chen, Y. Effect of cement composition on the expansion of heat-cured cement pastes. *Cem. Concr. Res.* **1995**, *25*, 853–862.
20. Martin, R.P. Analyse sur Structures Modèles des Effets Mécaniques de la Réaction Sulfatique Interne Du béton. Ph.D. Thesis, Université Paris-Est, Paris, France, 2010.
21. Al Shaama, M.; Lavaud, S.; Divet, L.; Nahas, G.; Torrenti, J.M. Influence of relative humidity on delayed ettringite formation. *Cem. Concr. Compos.* **2015**, *58*, 14–22. [CrossRef]
22. Graf, L. *Effect of Relative Humidity on Expansion and Microstructure of Heat-Cured Mortars*; Portland Cement Association: Skokie, IL, USA, 2007.
23. Sellier, A.; Multon, S. Chemical modelling of delayed ettringite formation for assessment of affected concrete structures. *Cem. Concr. Res.* **2018**, *108*, 72–86. [CrossRef]

24. Bouzabata, H.; Multon, S.; Sellier, A.; Houari, H. Swelling due Alkali-Silica reaction and delayed ettringite formation: Characterisation of expansion isotropy and effect of moisture conditions. *Cem. Concr. Compos.* **2012**, *34*, 349–356. [CrossRef]
25. Martin, R.P.; Bonnet, A.; Renaud, J.C.; Chlela, R.; Toutlemonde, F.; Sauvaget, C. Influence of moisture on the development of Delayed Ettringite Formation. *Mag. Concr. Res.* **2023**, *75*, 747–754. [CrossRef]
26. Escadeillas, G.; Aubert, J.; Segerer, M.; Prince, W. Some factors affecting delayed ettringite formation in heat-cured mortars. *Cem. Concr. Res.* **2007**, *37*, 1445–1452. [CrossRef]
27. Young, J.F. Humidity control in the laboratory using salt solutions—A review. *J. Appl. Chem.* **1967**, *17*, 241–268. [CrossRef]
28. Ulm, F.J.; Coussy, O.; Li, K.; Larive, C. Thermo-chemo-mechanics of ASR expansion in concrete structures. *ASCE J. Eng. Mech.* **2000**, *126*, 233–242. [CrossRef]
29. Nedjar, B.; Rospars, C.; Martin, R.P.; Toutlemonde, F. Benchmark Study Results: IFSTTAR. In *Diagnosis and Prognosis of AAR Affected Structures: State-of-the-Art Report of the RILEM TC 259-ISR*; Saouma, V.E., Ed.; Springer International Publishing: Berlin/Heidelberg, Germany, 2021; pp. 401–411.
30. Larive, C. *Apports Combinés de l'Expérimentation et de la Modélisation à la Compréhension de L'alcali-Réaction et de ses Effets Mécaniques, OA28*; Technical Report; Laboratoire Central des Ponts et Chaussées: Paris, France, 1998.
31. Malbois, M.; Nedjar, B.; Lavaud, S.; Rospars, C.; Divet, L.; Torrenti, J.M. On DEF expansion modelling in concrete structures under variable hydric conditions. *Constr. Build. Mater.* **2019**, *207*, 396–402. [CrossRef]
32. Jabbour, J. Étude multi-échelles de l'attaque sulfatique externe dans les structures en béton armé, Ph.D. Thesis, University Paris-Est, Marne-la-Vallée, France, 2019.